



THE OPTIMUM SPACING BETWEEN PARALLEL HEAT GENERATING BOARDS COOLED BY LAMINAR FORCED CONVECTION

Hafit Yüncü and Özgür Ekinci

Middle East Technical University, Department of Mechanical Engineering, 06531 ANKARA
hafit@metu.edu.tr

(Geliş Tarihi: 13. 06 2006)

Abstract: Laminar forced convection heat transfer in parallel heat generating board in fixed volume of electronic package is investigated numerically. The main objective of this study is to maximize the total rate of heat transfer from the package to the air that flows through it. The boards are equidistant and the constraint of the optimization procedure is the constant pressure drop maintained across the electronic package for varying spacing of the heat-generating boards. The optimal board spacing that maximizes the total heat transfer rate is determined. Board surfaces with both uniform temperature and uniform heat flux are considered. The results of the optimization procedure show that the type of thermal boundary condition practically has no effect on the optimal board-to-board spacing.

Keywords: Laminar forced convection, Electronic package, Optimal board spacing.

LAMİNER ZORLANMIŞ TAŞINIM İLE SOĞUTULAN ISI ÜRETEK PARALEL LEVHALAR ARASINDAKİ EN UYGUN ARALIĞIN BELİRLENMESİ

Özet: Bu çalışmada laminar zorlanış taşınım ile soğutulan sabit hacimli elektronik paket içerisine yerleştirilmiş paralel kartlardan ısı transferi sayısal olarak incelenmiştir. Çalışmanın amacı elektronik paketten maksimum ısı transferi için, kartlar arasındaki optimum aralığın belirlenmesidir. Optimum aralığın belirlenmesinde kartlar arasındaki aralıklar eşit varsayılmış, ve basınç düşümü de sabit alınmıştır. Kartlar arasındaki gelişmekte olan laminar hava akışı, kart yüzeylerinde sabit sıcaklık ve sabit ısı akışı ısı sınır şartlarında incelenmiştir. Sayısal çözümler laminar akışta optimum kart aralığının ısı sınır şartlara bağlı olmadığını göstermektedir.

Anahtar Kelimeler: Laminar zorlanmış taşınım, Elektronik paket, Optimum kart aralığı.

LIST OF SYMBOLS

a	Coefficient for discretization equations	U_{∞}	Coolant inlet velocity [m/s]
C_p	Specific heat of the fluid at constant pressure [kJ/(kg•K)]	u^*	Dimensionless velocity component in x-direction
d	Spacing between the parallel heat-generating boards [m]	v	Velocity component in y direction [m/s]
D_h	Hydraulic diameter [m]	v^*	Dimensionless velocity component in y-direction
d_{opt}	Optimum spacing [m]	x	Axial (stream-wise) coordinate in Cartesian system, [m]
H	Height of the electronic package [m]	x^*	Dimensionless axial coordinate
k	Thermal conductivity [W/(m•K)]	y	Cartesian coordinate across the cross section [m]
L	Length of the electronic package [m]	y^*	Dimensionless Cartesian coordinate across the cross section
Nu	Nusselt number	ΔP	Pressure drop in flow direction, Pa
P	Pressure [Pa]	ΔP^*	Dimensionless pressure drop in flow direction
P^*	Dimensionless pressure	Δx_i	Numerical grid spacing in x direction [m]
Pr	Prandtl number	Δy_j	Numerical, non-uniform grid spacing in y-direction [m]
Q	Total heat transfer rate per unit width of the package [W/m]	α	Thermal diffusivity [m ² /s]
q''_w	Wall heat flux [W/m ²]	μ	Dynamic viscosity coefficient [Pa•s]
Re	Reynolds number	ν	Kinematic viscosity [m ² /s]
T	Temperature [K]	θ	Dimensionless temperature
T_{∞}	Coolant inlet temperature [K]	θ_m	Dimensionless mean temperature
T_m	Mean temperature [K]	ρ	Density [kg/m ³]
T_w	Wall temperature [K]		
u	Velocity component in x direction [m/s]		

INTRODUCTION

In recent years, electronics has become increasingly important in all faces of modern life from biomedical devices to aerospace applications. Design of electronic packaging is multi-disciplinary in nature as it involves the solution of electrical, mechanical and thermal problems. In this study, the attention is placed on the later. During the last two-three decades, the need for more compact electronic equipment has increased the power density of electronic packages, and hence their heat dissipation rate (Yanagida, 1988). For example, during the past 30 years, printed circuit boards (PCB's) have gone from 4 to as many as 50 layers, line widths have been reduced from 0.25 to 0.05 mm and package densities have increased approximately 7 times (Bar-Cohen, 1994). If the individual element (chips) is taken into consideration, chip sizes have been reduced approximately from 100 to 1 μm while number of components in one chip has increased approximately from 1 to 10^5 (Kakaç, 1994).

To mount as many circuitry as possible in a given space requires shape optimization which is the most critical part of a thermal design. Shape optimization is the selection of the way in which components are arranged relative to each other in the finite space occupied by the package. The constraint of the optimization is the space, which is specified by the design specs and the two important design parameters are the cooling mode and the allowable upper temperature limit. The simplest cooling mode is single phase laminar flow in natural or forced convection. Although the allowable temperature vary from one to another applications, the failure rates increase by a factor of two for every 10 $^{\circ}\text{C}$ increment in operating temperature (Antonetti *et al.*, 1989). The task of the today's thermal engineers in the field of electronics is to maintain the component temperatures relatively low despite of these high heat fluxes.

Packaging constraints, electronic considerations, device or system operating modes lead to a variety of complex models for optimization. Horizontal two-dimensional channels formed by parallel plates, which are modeled either as uniform-flux or isothermal are well representative of different cases with an acceptable accuracy. Modeling of heat transfer from parallel plates is also the subject of this study.

The purpose of this work is to determine the optimum board spacing to maintain the component temperatures below the allowable temperature limit and maximize the total rate of heat transfer from the finite space occupied by the package. The coolant (air) is assumed to be forced to flow through the package and the flow is laminar.

The available literature on optimal spacing was reviewed most recently in Bejan (2000). Pioneering work by Tomimura and Fujii (1991) investigated the

mixed convection of laminar airflow between vertical parallel plates with discrete heat sources. A correlation that predicts the maximum temperature of each heat source within a practical accuracy was obtained. Bejan and Sciubba (1992) studied the optimal board-to-board spacing between parallel plates cooled by forced convection for the laminar flow in the entrance region. Study was based on solution with the order of magnitude analysis of basic equations. Results are supported with some sort of numerical solution obtained from empirical pressure drop. Later work by Mereu *et al.* (1993) is again for the laminar flow in entrance region of parallel plates. Governing equations were solved by a commercial finite element package, where the finite thickness of each board was taken into account.

In the present study, the working model is identical with the ones that appear in last two reviewed works. Here, the main novelty concerns the development of a numerical method to determine the optimal board spacing and maximum total heat transfer rate from a stack of parallel boards cooled by laminar forced convection of air.

WORKING MODEL AND GOVERNING EQUATIONS

The geometry of the electronic package is illustrated in Fig. 1. The fixed volume electronic package has height H , length L , and width W . A sufficiently large number of parallel electronic circuit boards, cooled by forced convection, are installed in the package. Since the thickness of generating boards is sufficiently smaller than the board spacing d , the thickness of the heat generating boards is neglected in the calculations.

The coolant (*air*) at temperature T_{∞} enters the package from the left with uniform velocity U_{∞} , flows through the board-to-board channels, and exits through the right opening. The pressure difference across the package ΔP , is prescribed. This is a representative model for installations in which the pressure difference is maintained by fan or pump. Since the electronic boards are sufficiently wide in the direction perpendicular to the plane, the flow is assumed two-dimensional and the heat-generating electronic boards are modeled as double sided and flush-mounted electronic chips.

Figure 2 represents the computational domain for this study. The equations that govern the process of forced convection for constant property incompressible flow (conservation of mass, momentum and energy) are expressed here in non-dimensional form in order to provide useful data in a computational investigation. The scaling parameters that represent the physical flow conditions are d , U_{∞} and T_{∞} . A two-dimensional (x, y) Cartesian system with the following non-dimensional variables is used

$$x^* = \frac{x}{d} \quad y^* = \frac{y}{d} \quad u^* = \frac{u}{U_\infty} \quad v^* = \frac{v}{U_\infty} \quad P^* = \frac{P}{\rho U_\infty^2}$$

$$\theta = \frac{T - T_\infty}{T_w - T_\infty} \quad (\text{For board surfaces with uniform temperature})$$

$$\theta = \frac{T - T_\infty}{q_w'' d / k} \quad (\text{For board surfaces with uniform heat flux})$$

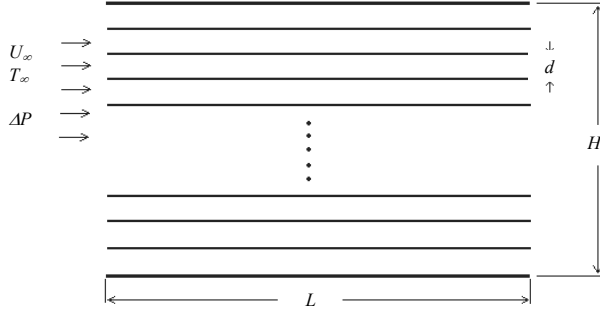


Figure 1. Stack of parallel heat generating boards cooled by forced convection.

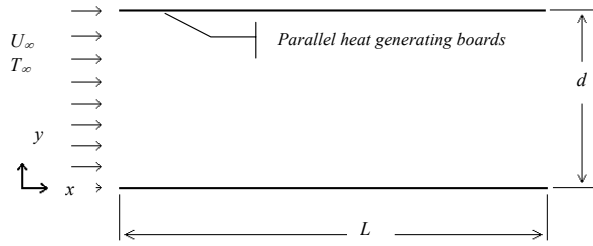


Figure 2. Computational domain.

In these expressions $u(x, y)$ and $v(x, y)$ are the velocity components, $P(x, y)$ stands for pressure and $T(x, y)$ for temperature.

In terms of these dimensionless parameters the governing equations can be expressed as:

Continuity

$$\frac{\partial u^*}{\partial x^*} + \frac{\partial v^*}{\partial y^*} = 0 \quad (1)$$

x - momentum

$$u^* \frac{\partial u^*}{\partial x^*} + v^* \frac{\partial u^*}{\partial y^*} = -\frac{\partial P^*}{\partial x^*} + \frac{2}{\text{Re}} \left(\frac{\partial^2 u^*}{\partial x^{*2}} + \frac{\partial^2 u^*}{\partial y^{*2}} \right) \quad (2)$$

y- momentum

$$u^* \frac{\partial v^*}{\partial x^*} + v^* \frac{\partial v^*}{\partial y^*} = -\frac{\partial P^*}{\partial y^*} + \frac{2}{\text{Re}} \left(\frac{\partial^2 v^*}{\partial x^{*2}} + \frac{\partial^2 v^*}{\partial y^{*2}} \right) \quad (3)$$

Energy

$$u^* \frac{\partial \theta}{\partial x^*} + v^* \frac{\partial \theta}{\partial y^*} = \frac{1}{\text{Pr}} \frac{2}{\text{Re}} \left(\frac{\partial^2 \theta}{\partial x^{*2}} + \frac{\partial^2 \theta}{\partial y^{*2}} \right) \quad (4)$$

In these equations the Reynolds number and the Prandtl number are defined as

$$\text{Re} = \frac{U_\infty 2d}{\nu} \quad (5a)$$

$$\text{Pr} = \frac{\rho n c_p}{k} \quad (5b)$$

Where ν, c_p, n and k are the fluid properties and are assumed to be constant.

The governing equations are elliptic and require boundary conditions to be prescribed around all boundaries. Four types of boundary are present: the symmetry plane, the board surface, and the inlet and outlet planes. There will be no flow across the symmetry plane, thus the velocity component v^* along the symmetry plane, and both the gradient of temperature and velocity component u^* across the symmetry plane are zero:

$$y^* = 1/2 \quad 0 < x^* < L/d; \quad v^* = 0, \quad \frac{\partial u^*}{\partial y^*} = 0, \quad \frac{\partial \theta}{\partial y^*} = 0 \quad (6)$$

Since the board surface is smooth, impermeable and with no slip, all velocity components are zero on it. Either uniform temperature or uniform heat flux boundary conditions have been applied.

$$y^* = 0; \quad 0 < x^* < L/d; \quad v^* = 0 \quad u^* = 0,$$

$$\theta = 1 \quad (\text{For board surfaces with uniform temperature})$$

$$\frac{\partial \theta}{\partial y^*} = -1 \quad (\text{For board surfaces with uniform heat flux})$$

(7)

Air at a uniform temperature T_∞ enters the computational domain through the inlet plane with uniform velocity U_∞ . Thus, the inlet boundary conditions are

$$x^* = 0; \quad 0 < y^* < 1/2; \quad u^* = 1 \quad v^* = 0 \quad \theta = 0 \quad (8)$$

If the length of the computational domain is sufficiently larger than the board spacing d , it is common practice to assume that the flow is perpendicular to the outlet plane and that the heat transfer on the outlet is purely by convection rather than by conduction. The boundary conditions become:

$$x^* = L/d \quad 0 < y^* < 1/2;$$

$$\frac{\partial v^*}{\partial x^*} = 0 \quad \frac{\partial u^*}{\partial x^*} = 0 \quad \frac{\partial \theta}{\partial x^*} = 0 \quad (9)$$

Since the given flow field must satisfy the continuity equation, the governing differential equations (momentum and energy equations) can be expressed in the form of a single elliptic differential equation of the form

$$\frac{\partial(u^* \phi)}{\partial x^*} + \frac{\partial(v^* \phi)}{\partial y^*} = \frac{\partial}{\partial x^*} \left(\Gamma \frac{\partial \phi}{\partial x^*} \right) + \frac{\partial}{\partial y^*} \left(\Gamma \frac{\partial \phi}{\partial y^*} \right) + S_\phi \quad (10)$$

where ϕ represents a generic, dependent field variable (u^* , v^* , or θ), Γ is a coefficient and S_ϕ is the source term. Their values are given in Table 1. Here too, the terms on the left-hand side of equation represent the convective terms; the first two terms on the right-hand side represent the diffusive terms and S_ϕ represents the source terms.

Table 1. Non-dimensional coefficients relating the governing equations of laminar forced convection to the general elliptic equation.

	ϕ	Γ	S_ϕ
<i>x - momentum</i>	u^*	$\frac{2}{\text{Re}}$	$-\frac{\partial P^*}{\partial x^*}$
<i>y - momentum</i>	u^*	$\frac{2}{\text{Re}}$	$-\frac{\partial P^*}{\partial y^*}$
<i>Energy</i>	θ	$\frac{2}{\text{Re Pr}}$	0

Since the governing equations can be expressed in a single form of a differential equation, a solution technique that is capable of solving the differential equation of this general form will also be suitable to handle the present problem. One such a numerical solution technique was developed by Patankar (1980), is based on a control volume-finite difference formulation, in which the above equations are integrated over the control volume that is part of the domain of interest and is constructed through the midpoints of the finite-difference mesh surrounding a point P where the values of the field variables are to be determined. The neighboring nodal points are labeled as compass indicators as N , S , E and W as shown in Figure 3.

During the integration a staggered grid arrangement is used and a central differencing scheme for the discretization of diffusion terms and a power-law scheme for the discretization of convective terms are employed. Assembling the integrated form of the

convective, diffusive and the source terms a set of discretized linear algebraic equation of the form

$$a_P \phi_P = a_E \phi_E + a_W \phi_W + a_N \phi_N + a_S \phi_S + b \quad (11)$$

is obtained. This equation, which is called finite volume equation, represents the influence of convection and diffusion at the four faces of control volume and source term on the value of the field variable ϕ at point P . a_E , a_W , a_N , and a_S are the neighboring coefficients. They represent influence of convection and diffusion, in terms of flow rate and conductance. The term b represents the integration of the source term over the cell. See Patankar (1980) for the details of this formulation.

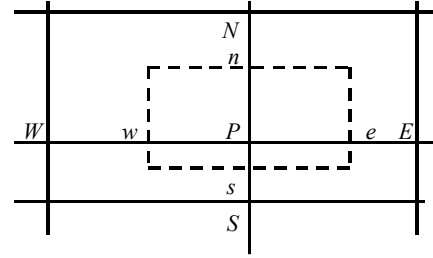


Figure 3. The domain for the discretization of general elliptic equation.

The discretized momentum equations, can be solved only when the pressure field is given or is somewhat estimated. Unless the correct pressure field is employed the resulting velocity field from the momentum equations will not satisfy the continuity equation. Such an imperfect velocity field (based on a guessed pressure field) can be improved and will progressively get closer to satisfying the continuity equation by applying the velocity and pressure corrections on the guessed values. The details of formulation of velocity and pressure corrections are given in Patankar (1980). After the flow field has been computed, the temperature distribution is found by solving the discretized energy equation.

The above numerical procedure is given the name SIMPLE, which stands for Semi-Implicit Method for Pressure-Linked Equations. It is an iterative method; the guessed pressure field is corrected after each iteration process, following the solution of discretized momentum equations. A line-by-line tri-diagonal matrix algorithm is applied to solve system of discretized equations while different under relaxation factors are used to prevent instability and divergence due to non-linearity in the Navier-Stokes equations (Eqs. (2) and (3)).

For deriving the discretization of conservation equations, the field of interest has been covered by an orthogonal grid network. The grid network consists of 36 uniform grid lines in x direction and 19 non-uniform grids lines in y direction. In the x direction, the spacing between grid lines was taken constant and equal to

$$x_i^* - x_{i-1}^* = \frac{l^*}{35} \quad 1 \leq i \leq 35 \quad (12)$$

where i is the number of grid lines in x direction. In the y direction, where a steep gradient of variable occurs, the spacing between the adjacent grid lines was varied according to the following relation.

$$y_j^* - y_{j-1}^* = \frac{j}{19 \times 18} \quad 1 \leq j \leq 19 \quad (13)$$

Where j is the number of grid lines in y direction. Figure 4 represents a part of such a grid, a typical node (i, j) , and the four surrounding nodes $(i-1, j)$, $(i+1, j)$, $(i, j-1)$ and $(i, j+1)$. Starting with a uniform inlet velocity, the flow solution takes about 150-200 iterations to converge.

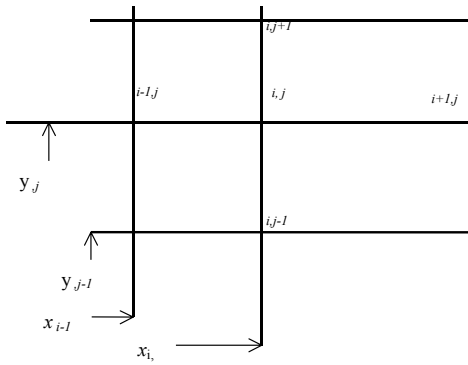


Figure 4. Spacing between grid lines.

A numerical code has been developed to perform the analysis presented in this study. The code is written in JAVA programming language. The program consisted of three main parts; the first part is for the calculation of coefficients, the second is the part that includes matrix solver and other routine operations, and the third part checks convergence, calculates new variables etc. In the iterative solutions, there is difference between the exact solution of the finite difference equations and the solution reached when the iteration scheme is stopped. For the iterative matrix solutions of x and y -momentum equations, fractional change in each dependent variable at each node was examined to determine the convergence by the following formula

$$\left| \frac{\phi^N - \phi^{N-1}}{\phi^N} \right|_{\max} \leq \eta \quad (14)$$

where ϕ^N is the value of the variable ϕ at the end of the N^{th} cycle and ϕ^{N-1} is its value of the $(N-1)^{\text{th}}$ cycle. η is the convergence criterion and is taken to be 0.0001 in this study.

For the pressure correction and for the residual of the continuity equation, absolute change at each node was examined to determine convergence.

$$|\phi^N - \phi^{N-1}|_{\max} \leq \eta \quad (15)$$

where η_c is the convergence criterion. η_c is taken as 0.00005 for the solutions of pressure correction equation and 0.00002 for the residual of continuity equation.

In order to confirm the validity and accuracy of solution method used in the current study, first dimensionless pressure drops for hydrodynamically developing laminar flow in a flat duct are calculated. Calculated dimensionless pressure drops are compared with the dimensionless pressure drops that were evaluated by using correlations developed by Shah and London (1987):

$$f_{app} \text{Re} = \frac{3.44}{(x^+)^{1/2}} + \frac{24 + 0.674/(4x^+) - 3.44/(x^+)^{1/2}}{1 + 0.000029(x^+)^{-2}} \quad (16)$$

This comparison is shown in Figure 5. Where the apparent friction factor, f_{app} and dimensionless coordinate x^+ are employed according to their definitions respectively,

$$f_{app} \text{Re} = \frac{\Delta P^*}{4x^+} \quad (17)$$

$$x^+ = \frac{L}{D_h \text{Re}} = \frac{L}{2d \text{Re}} \quad (18)$$

Examination of Figure 5 reveals that the results of present numerical study are in excellent agreement with the aforementioned correlation.

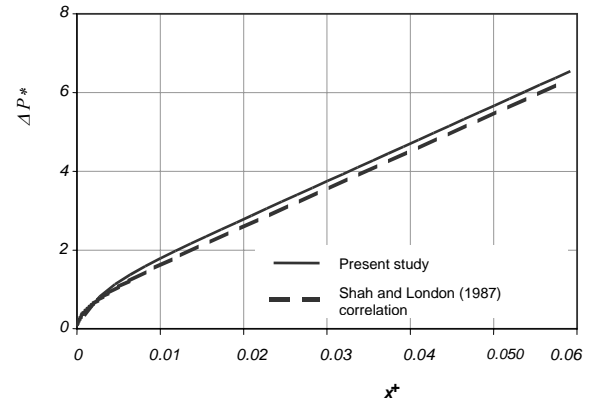


Figure 5. Dimensionless pressure drop for hydrodynamically developing flow in a flat duct.

There are a large number of experimentally based correlations for Nusselt number in literature for simultaneously developing laminar flow in flat duct. For assessing the accuracy of current computational approach, calculated Nusselt numbers for board surfaces with uniform temperature are also compared with those reported by Shah and Bhatti (1987):

$$Nu_{x,T} = 7.55 + \frac{0.024(x^{++})^{-1.14} [0.0179 \text{Pr}^{0.17} (x^{++})^{-0.64} - 0.14]}{[1 + 0.0358 \text{Pr}^{0.17} (x^{++})^{-0.64}]^2} \quad (19)$$

For dimensionless presentation, the Nusselt number and axial coordinate x^{++} are defined by,

$$Nu_x = \frac{h_x D_h}{k} = \frac{h_x 2d}{k} \quad (20)$$

$$x^{++} = \frac{x}{D_h Pe} = \frac{x}{2d Re Pr} \quad (21)$$

and the result of the comparison is displayed in Fig 6. The numerical results are in excellent agreement with the results of correlation reported by Shah and Bhatti (1987). The average relative deviation is less than 6%. These agreements confirm the validity of numerical technique used in this study.

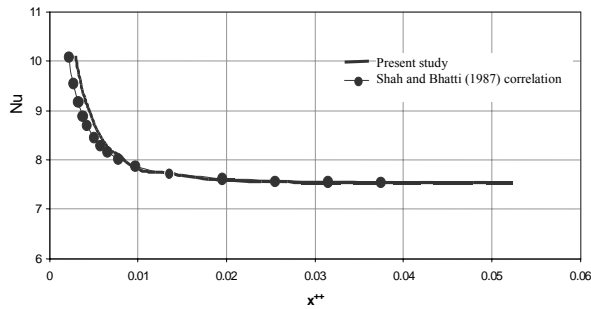


Figure 6. Local Nusselt number for simultaneously developing laminar flow in a flat duct with constant wall temperature boundary condition.

THE OPTIMAL BOARD-TO- BOARD SPACING

Board Surfaces with Uniform Temperature

Consider now the problem of determining the optimal number of isothermal plates (constant temperature boundary condition) in a space (package) cooled by forced convection. The optimal number of isothermal plate means to find the optimal board-to-board spacing for maximum heat transfer rate extracted by the coolant (air). The heat transfer rate through a single channel can be formulated as

$$\dot{Q}_{single} = \dot{m} C_p (T_{me} - T_{\infty}) \quad (22)$$

where \dot{m} is the mass flow rate through the single channel, C_p is the specific heat of air at constant pressure, T_{∞} is the inlet temperature and T_{me} is the outlet mean temperature. The mass flow rate through the single channel is expressed per unit length in the direction perpendicular to the flow.

If the number of channels is expressed as $N = H/d$, then the total heat transfer rate from the package may be expressed as

$$\dot{Q} = \dot{m} C_p (T_{me} - T_{\infty}) \frac{H}{d} \quad (23)$$

in which

$$\dot{m} = \rho U_{\infty} d \quad (24)$$

$$U_{\infty} = \frac{Re v}{2d} = \frac{Re v}{2(d/L) L} \quad (25)$$

$$T_{me} - T_{\infty} = (T_w - T_{\infty}) \theta_{me} \quad (26)$$

Substituting Eqs. (24), (25) and (26) into Eq. (23) the heat transfer rate from the package can be calculated as,

$$\dot{Q} = \rho \frac{Re v}{2} C_p (T_w - T_{\infty}) \frac{H}{d} \theta_{me} \quad (27)$$

The resulting expression can be nondimensionalized as

$$\frac{\dot{Q} L}{\rho C_p H (T_w - T_{\infty}) v} = \frac{1}{2} \frac{Re \theta_{me}}{(d/L)} \quad (28)$$

Since L, H, v, C_p, ρ and $(T_w - T_{\infty})$ are fixed our job is to maximize the quantity on the right hand side of this last expression (objective function), subject to the constraint,

$$\Delta P = Constant \quad (29)$$

Board Surfaces with Uniform Heat Flux

The total heat transfer rate from an $L \times H$ space filled by a stack of $N = H/d$ number of parallel boards with uniform heat flux q_w'' on both surfaces is

$$\dot{Q} = 2 N q_w'' L \quad (30)$$

and that the maximum temperature of the board, which occurs at its trailing edge, is

$$\theta_{w_{max}} (x^* = \frac{L}{d}, y^* = 0) = \frac{T_{w_{max}} - T_{\infty}}{q_w'' d / k} \quad (31)$$

where $T_{w_{max}}$ denotes the local wall temperature at down stream, at distance L from the inlet. Combining Equations (30) and (31) yields

$$\dot{Q} = \frac{2k \left(\frac{H}{L} \right) (T_{w_{max}} - T_{\infty})}{\left(\frac{d}{L} \right)^2 \theta_{w_{max}}} \quad (32)$$

where $T_{w_{max}}$ is the maximum allowable surface temperature. The total heat transfer rate can be calculated by recognizing the thermal conductivity of the fluid

$$k = \frac{\rho C_p \nu}{Pr} \quad (33)$$

This yields

$$\frac{\dot{Q}L}{\rho C_p H(T_{w_{max}} - T_{\infty})\nu} = \frac{2}{Pr} \frac{1}{\theta_{max} (d/L)^2} \quad (34)$$

where L , H , ν , C_p , and ρ are given. Therefore, the objective is to maximize \dot{Q} while keeping the maximum allowable surface temperature $T_{w_{max}}$ below safe level or to maximize the quantity $\frac{2}{Pr} \frac{1}{\theta_{max} (d/L)^2}$ on the right hand side of Eq. (34) subject to the same constraint,

$$\Delta P = Constant \quad (35)$$

The constraint can now be nondimensionalized as

$$\Delta P \frac{4L^2}{\rho \nu^2} = \Delta P^* \frac{Re^2}{(d/L)^2} \quad (36)$$

in which L , ρ , ν and ΔP are fixed. Therefore, the constraint of optimization then, can be written in term of the dimensionless group on the right hand side of Eq. (36)

$$\Delta P^* \frac{Re^2}{(d/L)^2} = Constant \quad (37)$$

MAXIMIZATION PROCEDURE

The maximization procedure consists of calculating the dimensionless heat transfer rate from the package, $\dot{Q}L/\rho C_p H(T_w - T_{\infty})\nu$ or $\dot{Q}L/\rho C_p H(T_{w_{max}} - T_{\infty})\nu$ for constant temperature and constant heat flux boundary condition respectively. These are calculated from Eq. (28) or Eq. (34) for the values of constrain $\Delta P^* \frac{Re^2}{(d/L)^2} = 2.193 \times 10^7, 3.834 \times 10^7, 5.745 \times 10^7, 7.881 \times 10^7, 9.177 \times 10^7, 1.225 \times 10^8, 2.226 \times 10^8, 4.678 \times 10^8, 1.359 \times 10^9, 2.577 \times 10^9$ and 5.468×10^9 by the following procedure.

Assumed first is the value of (d/L) , which played the role of parameter. For each value of (d/L) the sequence of numerical calculations can be stated as

- Guess the Reynolds number ($Re \leq 2300$)
- Calculate the dimensionless pressure drop ΔP^* from Eq. (37)
- Solve the continuity and momentum equations Eqs. (1), (2) and (3) to obtain dimensionless velocity components u^*, v^*

- Calculate the dimensionless pressure drop ΔP^* from the velocity pressure correction relation. Treat the calculated dimensionless pressure drop as a new guessed dimensionless pressure drop, return the first step and repeat the whole procedure until a converged solution is obtained
- Solve the energy equation Eq. (4) to obtain the temperature distribution for constant temperature or constant heat flux boundary condition.
- Calculate the dimensionless heat transfer rate from the package from Eq. (28) when the board surface temperature is assumed uniform or from Eq. (34) when the board surface is modeled as uniform heat flux.

In this way emerge numerically the one to one relationship between the dimensionless heat transfer rate from the package $\dot{Q}L/\rho C_p H(T_w - T_{\infty})\nu$, or $\dot{Q}L/\rho C_p H(T_{w_{max}} - T_{\infty})\nu$, dimensionless pressure drop $\Delta P \frac{4L^2}{\rho \nu^2}$ and the parameter (d/L) In Figures (7) and (8) the variation of $\dot{Q}L/\rho C_p H(T_w - T_{\infty})\nu$ and $\dot{Q}L/\rho C_p H(T_{w_{max}} - T_{\infty})\nu$ are plotted as a function of (d/L) for different values of $\Delta P \frac{4L^2}{\rho \nu^2}$. From Figs (7) and (8) it can be observed that at a given dimensionless pressure drop, heat transfer rate from the package ($\dot{Q}L/\rho C_p H(T_w - T_{\infty})\nu$ or $\dot{Q}L/\rho C_p H(T_{w_{max}} - T_{\infty})\nu$) first increases up to a maximum value and then starts decreasing. The value of the parameter (d/L) at which the heat transfer rate is maximized is called optimal board-to-board spacing d_{opt} . The optimal board spacing (L / d_{opt}) for the given pressure drop $\Delta P \frac{4L^2}{\rho \nu^2}$ is given in Fig. 9. This figure shows that the optimal board-to-board spacing is almost insensitive to the type of boundary condition used. A curve is also provided to fit the data in Fig. 9 to demonstrate the trend of the numerical data points. The equation of this curve is obtained by square regression method as

$$\frac{L}{d_{opt}} = 0.217 \left[\Delta P \frac{4L^2}{\rho \nu^2} \right]^{1/4} \quad (38)$$

For air flow, recognizing that $Pr = \frac{n}{a} = 0.72$, Eq. (38) can be written as

$$\frac{d_{opt}}{L} = 3.00 \left[\frac{\Delta P L^2}{\alpha \mu} \right]^{1/4} \quad (39)$$

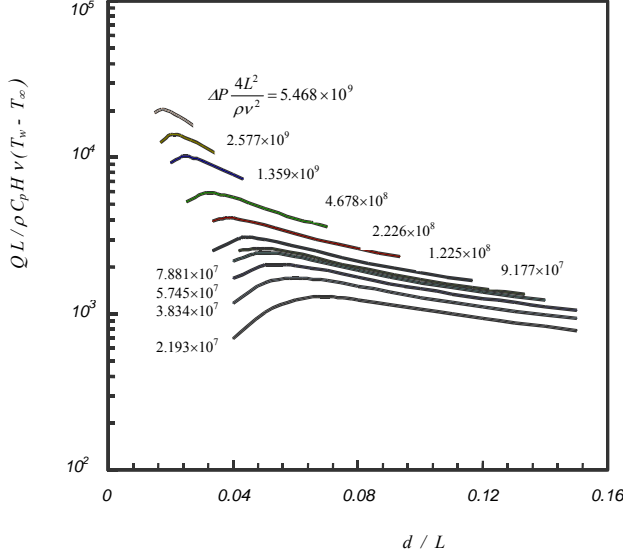


Figure 7. The total heat transfer rate versus board-to-board spacing for a space filled by a stock of parallel boards with both surfaces isothermal ($Pr=0.72$).

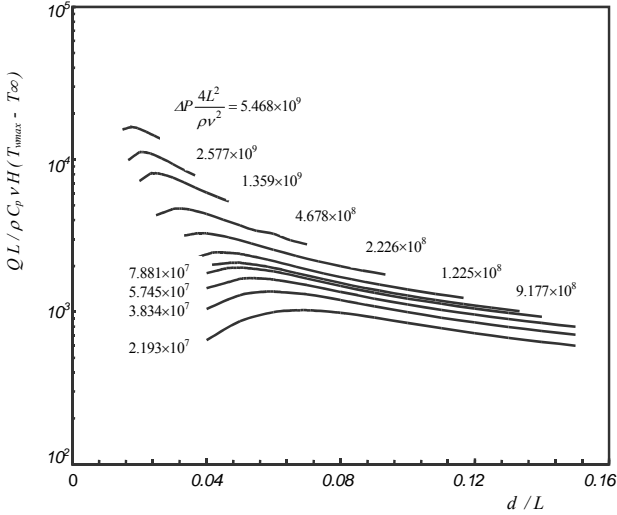


Figure 8. The total heat transfer rates versus board-to-board spacing for a space filled by a stock of parallel boards with uniform heat flux on both surfaces ($Pr=0.72$).

The fitted curve indicates that the optimal board spacing is proportional to $L^{1/2}$ and inversely proportional to $\Delta P^{1/4}$. The properties of coolant affect the optimal board-to-board spacing through the group of properties $(\alpha\mu)^{1/4}$. In convective heat transfer literature,

the dimensionless pressure difference group $\left[\frac{\Delta PL^2}{\alpha\mu}\right]$ was termed as Bejan number by Bhattacharjee and Grosshandler (1988).

The optimal dimensionless board spacing for air flow ($Pr=0.72$ as in this work) is 10% greater than the order of magnitude estimate given in Bejan and Scuibba (1992)

$$\frac{d_{opt}}{L} \cong 2.730 \left[\frac{\Delta PL^2}{\alpha\mu} \right]^{-1/4} \quad (40)$$

and 1% less than the result of numerical solution obtained from empirical pressure drop and reported in Bejan and Scuibba (1992).

$$\frac{d_{opt}}{L} = 3.033 \left[\frac{\Delta PL^2}{\alpha\mu} \right]^{-1/4} \quad (41)$$

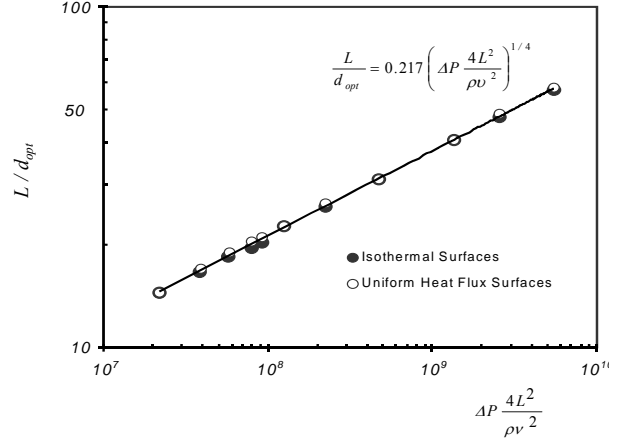


Figure 9. The optimal spacing versus pressure drop for a space filled with by a stack of parallel boards (Isothermal and uniform heat flux surfaces).

The maximum total heat transfer rate from a space filled with stack of parallel boards, is the value of heat transfer rate that corresponds the optimal spacing at a given pressure drop. In Fig. 10, the variation of maximum total heat transfer rate as a function of (L/d_{opt}) for boards with both isothermal surface is plotted. A curve is also provided to fit the numerical data in Fig 10. The equation of this curve is

$$\frac{\dot{Q}_{max} L}{\rho C_p H (T_w - T_{\infty}) v} = 6.05 \left(\frac{L}{d_{opt}} \right)^2 \quad (42)$$

In Fig.11, the variation of maximum total heat transfer rate as a function of (L/d_{opt}) is plotted for stack of parallel boards with uniform heat flux on both surfaces and the following functional form is selected as the best to represent these numerical data.

$$\frac{\dot{Q}_{max} L}{\rho C_p H (T_{w_{max}} - T_{\infty}) v} = 4.52 \left(\frac{L}{d_{opt}} \right)^2 \quad (43)$$

Substituting now, Eq. (38) into Eqs. (42) and (43) the overall thermal conductance of an air-cooled package becomes

$$\frac{\dot{Q}_{max} L}{kH(T_{w_{max}} - T_{\infty})} = 0.483 \left(\frac{\Delta PL^2}{\alpha\mu} \right)^{1/2} \quad (44)$$

$$\frac{\dot{Q}_{\max} L}{kH(T_{w_{\max}} - T_{\infty})} = 0.365 \left(\frac{\Delta PL^2}{\alpha\mu} \right)^{1/2} \quad (45)$$

for isothermal and uniform heat flux boundary conditions, respectively.

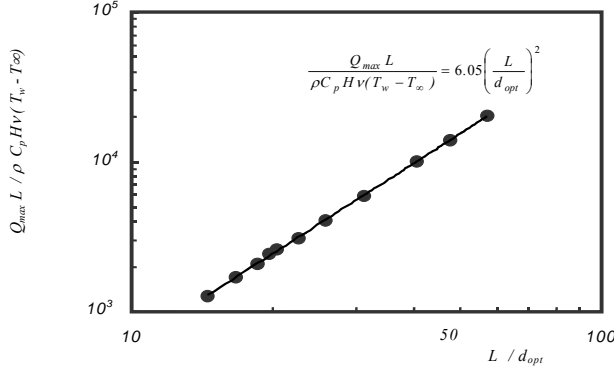


Figure 10. The optimal board-to-board spacing versus maximum heat transfer (Pr=0.72, Isothermal surfaces).

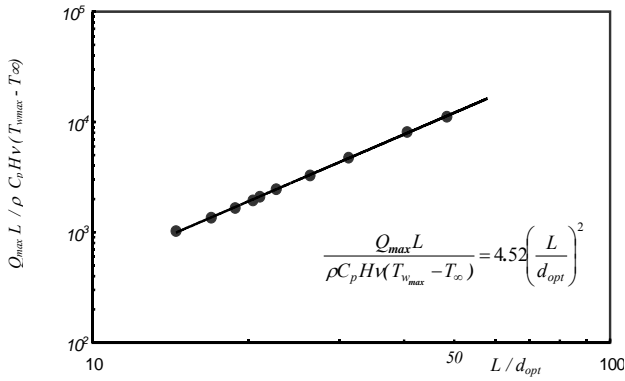


Figure 11. The optimal board-to-board spacing versus maximum heat transfer (Pr=0.72, Uniform heat flux surfaces).

The maximum total heat transfer rate is proportional to maximum allowable temperature difference between board and coolant inlet ($(T_w - T_{\infty})$ or $(T_{w_{\max}} - T_{\infty})$), height of the electronic package H , and square root of pressure drop $\Delta P^{1/2}$. When the allowable surface temperature is the same for both cases the maximum total heat transfer rate for board surfaces, which are isothermal, is 25% higher than that of uniform heat flux condition. This result is to be expected because the temperature of the isothermal surface is equal to the allowable surface temperature over its entire length while the temperature of the uniform-flux surface reaches to the allowable surface temperature only at its trailing edge.

According to the results of the numerical solution obtained from empirical pressure drop and reported in Bejan and Scuibba (1992) the thermal conductance for isothermal and uniform heat flux boundary conditions are

$$\frac{\dot{Q}_{\max} L}{kH(T_{w_{\max}} - T_{\infty})} = 0.479 \left(\frac{\Delta PL^2}{\alpha\mu} \right)^{1/2} \quad (46)$$

$$\frac{\dot{Q}_{\max} L}{kH(T_{w_{\max}} - T_{\infty})} = 0.371 \left(\frac{\Delta PL^2}{\alpha\mu} \right)^{1/2} \quad (47)$$

The numerical results of this study recommend something very similar. However, the maximum heat transfer rate calculated from Eq. (43) is 23% below the maximum value obtained by the order of magnitude estimate based on the intersection of asymptotes method developed in Bejan and Scuibba (1992) and is given by

$$\frac{\dot{Q}_{\max} L}{kH(T_{w_{\max}} - T_{\infty})} \leq 0.620 \left(\frac{\Delta PL^2}{\alpha\mu} \right)^{1/2} \quad (47)$$

CONCLUSION

The objective of this paper is to predict the optimal spacing for parallel heat generating board in a fixed volume of electronic package (stack) with prescribed pressure drop and cooled by laminar forced convection. The fixed pressure drop assumption is an acceptable model for installations in which several parallel packages receive their coolant from the same plenum. The pressure in the plenum is maintained by a fan or, in the case of a liquid coolant, by a pump. The fan or pump may be located upstream or downstream of the packages those are being cooled by laminar forced convection. Board surfaces with uniform temperature and uniform heat flux are considered. The optimal spacing which is the value of board-to-board spacing that correspond maximum total heat transfer rate from a package of parallel boards is not practically affected by the thermal boundary condition and is given by the relation.

$$\frac{d_{opt}}{L} = 3.00 \left[\frac{\Delta PL^2}{\alpha\mu} \right]^{1/4} \quad (48)$$

The optimal board-to-board spacing is directly proportional to $L^{1/2}$ and the property group $(\mu\alpha)^{1/4}$ and inversely proportional to $\Delta P^{1/4}$. These optimal results are obtained by complete numerical simulation of the flow and temperature fields in each channel of a fixed volume of electronic package. The results are valid when the flow is laminar. This condition acts as constraint on the pressure drop that is maintained constant across each channel.

REFERENCES

Antonetti, W.V., Oktay, S. and Simons, E.R., Heat Transfer in Electronic Packages, *Microelectronics Packaging Handbook*, Gomory, E.R. (ed), Library of Congress Cataloging in Publication Data, USA, 1989.

- Bar-Cohen, A., Trends in the Packaging of Computer Systems, *Cooling of Electronic Systems*, Kakaç, S., Yüncü H. and Hijikata K. (eds.), Kluwer Academic Publishers, Netherlands, 17-45, 1994.
- Bejan A., *Shape and Structure, From Engineering to Nature*, Cambridge University Press, Cambridge, UK, 2000.
- Bejan, A. and Sciubba, E., The Optimal Spacing of Parallel Plates Cooled by Forced Convection, *International Journal of Heat and Mass Transfer*, 35, 3259-3264, 1992.
- Bhattacharjee, S. and Grosshandler, W.L., The formation of a wall jet near a high temperature wall under micro gravity environment, *ASME HTD*, 96, 711-716, 1988.
- Kakaç, S., Introduction to ASI on Cooling of Electronic Systems, *Cooling of Electronic Systems*, Kakaç, S., Yüncü H. and Hijikata K. (eds.), Kluwer Academic Publishers, Netherlands, 1-15, 1994.
- Mereu, S., Sciubba, E. and Bejan, A., The Optimal Cooling of a Stack of Heat Generating Boards with Fixed Pressure Drop, Flow rate or Pumping Power, *International Journal of Heat and Mass Transfer*, 36, 3677-3686, 1993.
- Patankar, S.V., *Numerical Heat Transfer and Fluid Flow*, Hemisphere Publication Corporation, Washington, 1980.
- Shah, R.K. and London, A.L., Laminar Flow Forced Convection in Ducts, (cited in) Shah, R. K. and Bhatti, M. S., Laminar Convective Heat Transfer in Ducts, *Handbook of Single-Phase Convective Heat Transfer*, Kakaç, S., Yüncü H. and Hijikata K. (eds.), John Wiley & Sons, USA, 1987.
- Shah, R.K. and Bhatti, M.S., Laminar Convective Heat Transfer in Ducts, *Handbook of Single-Phase Convective Heat Transfer*, Kakaç, S., Yüncü H. and Hijikata K. (eds.), John Wiley & Sons, USA, 1987.
- Tomimura, T. and Fujii, M, Mixed Convection Heat Transfer from Vertical Parallel Plates with Discrete Heat Sources, *Transactions JSME*, 57 (534), 676-681, 1991.
- Yanagida, T., A Method for Calculating the Temperature Distribution of IC Packages on a PCB (Part I, Temperature Distribution in the Thermal Wake of an IC Package), *Transactions JSME*, 54 (503), 1730-1735, 1988.